The Astronomical Journal, 125:3111–3121, 2003 June

THE LUMINOSITY FUNCTION OF THE LARGE MAGELLANIC CLOUD GLOBULAR CLUSTER NGC 1866

E. Brocato,[1] V. Castellani,[2,3] E. Di Carlo,[1] G. Raimondo,[1,4] and A. R. Walker[5]

Received 2002 December 13; accepted 2003 February 19

ABSTRACT

We present *Hubble Space Telescope VI* photometry of the central region of the Large Magellanic Cloud cluster NGC 1866, reaching magnitudes as faint as $V = 27$. We find evidence that the cluster luminosity function shows a strong dependence on the distance from the cluster center, with a clear deficiency of low-luminosity stars in the inner region. We discuss a *global* cluster luminosity function as obtained from stars from all parts of the investigated region, which appears in impressive agreement with the prediction from a Salpeter mass distribution. We also revisit the use of NGC 1866 as a probe for determining the efficiency of core overshooting and conclude that a definitive answer to this question is not possible from this cluster.

Key words: color-magnitude diagrams — galaxies: star clusters — Magellanic Clouds — stars: evolution — stars: luminosity function, mass function

1. INTRODUCTION

NGC 1866 is a Large Magellanic Cloud (LMC) stellar cluster that is an extragalactic counterpart of young Galactic clusters such as the Pleiades, but with a much richer stellar population. It is probably one of the most massive objects formed in the LMC during the last 3 Gyr, with its total mass estimated as $M_{\rm tot} = (1.35 \pm 0.25) \times 10^5\ M_\odot$ by Fischer et al. (1992). Because of that richness, it presents a statistically significant sample of He-burning giants (more than 100 compared with none in the Pleiades), allowing the testing of predictions by stellar evolution models concerning late evolutionary phases in intermediate-mass stars, i.e., in stars with masses on the order of $\sim$4–5 $M_\odot$ (Arp & Thackeray 1967; Becker & Mathews 1983, hereafter BM83; Chiosi et al. 1989, hereafter C89; Brocato et al. 1989, hereafter B89; Testa et al. 1999, hereafter T99; Barmina, Girardi, & Chiosi 2002, hereafter BGC02).

The cluster dynamical mass has recently been investigated by van den Bergh (1999), who by a comparison of the cluster integrated photometry with the velocity dispersion measured by Fischer et al. (1992) found a very high mass-to-luminosity ratio ($M/L_V = 0.42$ in solar units), suggesting the possible occurrence of an unusual mass spectrum, much steeper than Salpeter's distribution (Salpeter 1955), and concluded that "clearly it would be of great interest to obtain deep *HST* photometry of this cluster to confirm this conclusion."

At about the same time, we were obtaining V and I *HST* images of the cluster, aiming to extend previous investigations to fainter magnitudes, as well as to reveal for the first time the stellar population right to the cluster center. In a previous paper (Walker et al. 2001, hereafter Paper I), we presented the first results of this *HST* photometry, discussing the color-magnitude diagram (CMD) location of the cluster main sequence (MS) in connection with the problem of the LMC distance modulus. In the present paper, we will use data corrected for completeness and field contamination to derive a new stellar luminosity function that extends to fainter than $V = 25$ mag. In § 2, we present the data reductions, and the derived luminosity function is studied in § 3. The constraints on the initial mass function (IMF) are discussed in § 4. Section 5 is devoted to a reexamination of the problem of overshooting in modeling the convective cores of stars. Final remarks close the paper.

2. THE OBSERVATIONS

The Wide Field Planetary Camera 2 (WFPC2) images of NGC 1866 were collected as part of the *Hubble Space Telescope* program GO-8151. Two telescope pointings were obtained, the first with the cluster core centered on the PC, the second with NGC 1866 at the center of the WF3 camera. This choice allows us to perform two independent data reductions and to make internal checks on the reproducibility and reliability of the results. The exposure times for the two selected filters F555W and F814W are given in Table 1, together with other observation details. The three sets of exposure times allow us to cover the high dynamic range of brightness of the cluster stars with good overlap between sets.

The WFPC2 mosaics of the two fields are presented in Figure 1 as observed in the medium-exposure images with filter F814W, whereas Figure 2 compares the present PC-centered fields with fields covered in previous ground-based observations.

The removal of cosmic rays and the photometry has been performed using the package HSTphot as developed by Dolphin (2000a) and according to the recipe outlined by the author. The most recent version of the HSTphot package has been used, which allows the simultaneous photometry of a set of images obtained by dithered multiple exposures,

[1] Osservatorio Astronomico di Teramo, via M. Maggini, I-64100 Teramo, Italy; brocato@te.astro.it, dicarlo@te.astro.it, raimondo@te.astro.it.

[2] Sezione di Ferrara, via Paradiso 12, I-44100 Ferrara, Italy.

[3] Osservatorio Astronomico di Roma, INAF, via di Frascati 33, I-00040 Monte Porzio Catone, Italy; vittorio@mporzio.astro.it.

[4] Dipartimento di Fisica, Università La Sapienza, P. Le Aldo Moro 2, I-00185 Roma, Italy.

[5] Cerro Tololo Inter-American Observatory, National Optical Astronomy Observatory, Casilla 603, La Serena, Chile; awalker@noao.edu. NOAO is operated by the Association of Universities for Research in Astronomy, Inc., under cooperative agreement with the National Science Foundation.

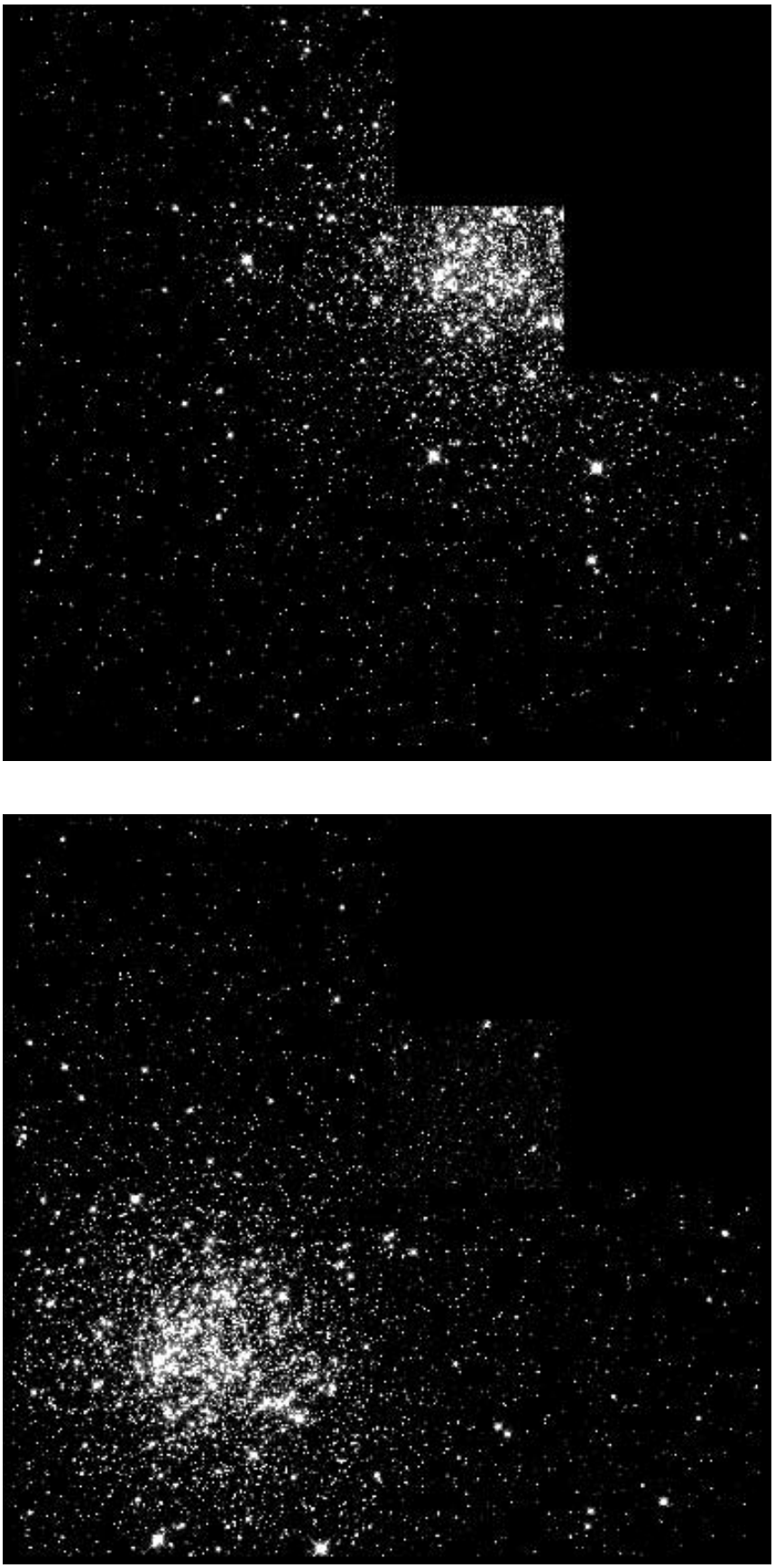

FIG. 1.—LMC cluster NGC 1866 as observed with WFPC2/*HST*. *Top*: PC-centered pointing for the 50 s exposures with the filter F814W is shown. *Bottom*: As in the left panel, but the WF3-centered pointing for the 50 s exposures with the filter F814W is shown.

TABLE 1
LOG OF THE OBSERVATIONS

Pointing	Data Set (name)	Filter	Exposure Time (s)	R.A. (J2000.0)	Decl. (J2000.0)	Position Angle (deg)
PC centered.....	u5dp510	F555W	4 × 8	05 13 43.28	−65 28 12.3	126.389
			8 × 60			
		F814W	4 × 5			
			8 × 50			
WF3 centered.....	u5dp020	F555W	4 × 8	05 13 33.07	−65 27 27.8	125.311
			8 × 60			
			4 × 500			
		F814W	4 × 5			
			8 × 50			
			2 × 500			
			2 × 600			

NOTES.—Coordinates refer to center of the PC and data set names refer to *HST* archive catalog.

as is our case. Each frame has been preprocessed according to the standard *HST* pipeline making use of the latest available calibrations, which are expected to provide the most accurate and stable results.

Following Dolphin (2000a), we used the subroutine MASK to take advantage of the accompanying data quality images by removing bad columns and pixels, charge traps, and saturated pixels. The same procedure is also able to properly solve the problem of the vignetted regions at the border of the chips. The CRMASK subroutine uses the available frames to clean the cosmic rays.

One of the advantages of HSTphot is that it allows use of point-spread functions (PSFs) that are computed directly to reproduce the shape details of star images as obtained in the different regions of the WFPC2. For this reason, we adopt the PSF-fitting option on the HSTphot routine, rather than use aperture photometry.

A particular difficulty in attempting to do photometry on these frames is the detection of fictitious objects, mainly located around the bright, very saturated stars on the medium and long exposures. These objects resemble the faint stars we are trying to measure, therefore we developed a procedure to get rid of the former, as follows. We selected all the stars located along *suspected* curves, as given by (1) circular distribution of objects around ($d \leq 30$ pixels) bright-saturated stars and (2) alignments (within 2 pixels) along lines centered on bright-saturated stars with an angle of 45° and at distances less than 49 pixels. Our algorithm rejected 7% of objects on the WF3 frames and 6% on the PC-centered frames.

Additionally, the HSTphot photometry routine returns various data quality parameters that can aid in the removal of spurious objects, we found the most useful of these to be the object classification parameter, which, in addition to the objects rejected by our algorithm as described above, found 13% of objects for the WF3-centered and 8% for the PC-centered frames to be spurious. The sharpness parameter would mainly find objects fainter than $V \sim 25$, presumably faint galaxies and stars with low S/N, while the χ and roundness parameters do not significantly improve the photometric results. We find that using our method combined with the HSTphot object classification parameter is a very effective method to identify fictitious objects.

In conclusion, by analyzing the list of objects provided by the output files of HSTphot, we find that the percentage of identified spurious objects is 20% and 14% for the WF3-centered and PC-centered data, respectively. This difference is not surprising, since the intensity of the saturation effects, the major effect responsible for generating spurious objects, depends on the exposure times, which are different between the two sets of data.

The results of all these selections are shown on Figure 3 where the CMDs of the rough photometry are compared with the CMDs as obtained after our selection. The CMDs show all the evolved stars located in the observed area. Within the box defined as $V = 17.4$–15.2 and $0.3 \leq (V-I) \leq (23.7 - V)/5$, we find a number of red giant (RG)[6] stars $N_{\rm RG} = 128$ and $N_{\rm RG} = 153$, respectively, for

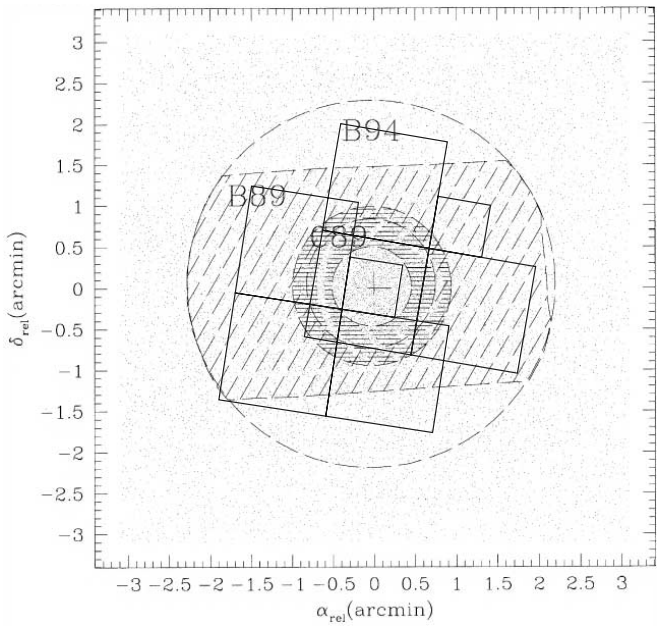

FIG. 2.—Present explored field of NGC 1866 compared with Fig. 7 of T99 in which their observations and previous ones (B89, C89, and B94) from ground telescopes are plotted.

[6] We are aware that the box also includes "blue" stars populating the loop region during the core He-burning phase. In this paper, we will use the terms "RG stars" and "He-burning giants" interchangeably.

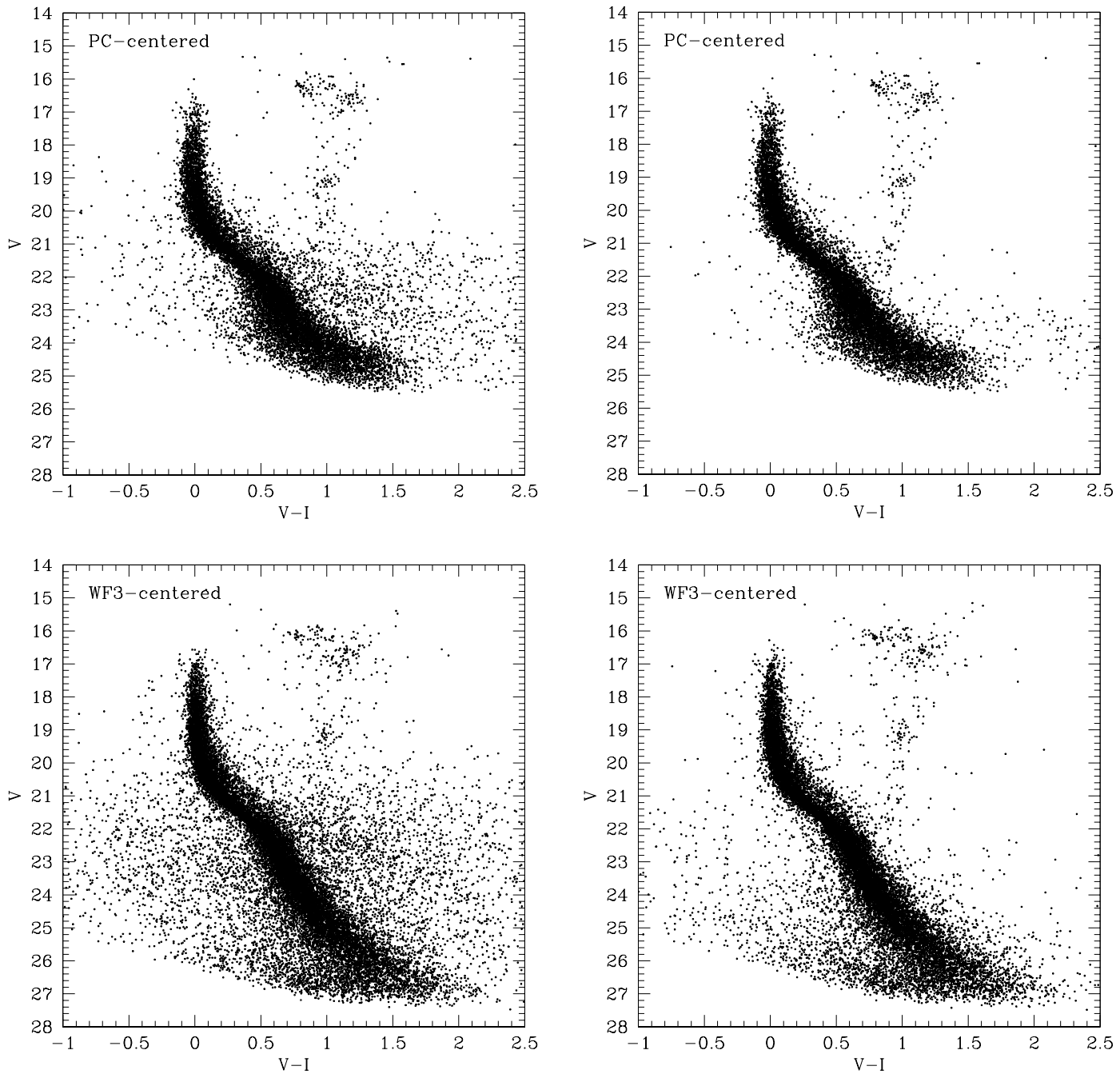

FIG. 3.—*Top*: PC-centered data set before (*left*) and after applying all the corrective procedures (*right*). *Bottom*: Same as above, but for the WF3-centered CMDs.

the PC-centered and WF3-centered data sets. We also note that the CMD clearly shows the presence of numerous evolved field giants in the LMC itself.

Charge transfer efficiency corrections and calibrations to the standard *VI* system were obtained directly by HSTphot routines, as documented by Dolphin (2000b). Figure 4 shows the uncertainties of photometry as a function of the magnitude for the two filters. Completeness has been evaluated by distributing artificial stars of known positions and magnitudes, in selected circular regions around the cluster center. The adopted procedure allows the distribution of stars with similar colors and magnitudes, as in the real CMD. The resulting completeness functions are shown in Figure 5 for the two sets of data and for the two selected filters. As expected, in both samples (WF3 and PC), the limiting magnitude for completeness decreases when moving from the periphery toward the cluster center.

To estimate the contamination by Galactic foreground stars, we used the tabulation by Ratnatunga & Bahcall (1985). We expect negligible MS contamination. Only 1.5 Galactic foreground stars are expected to be present in the region of the field red clump, while only 0.8 in the cluster RG region. Thus, we conclude that most contamination is due to LMC field stars.

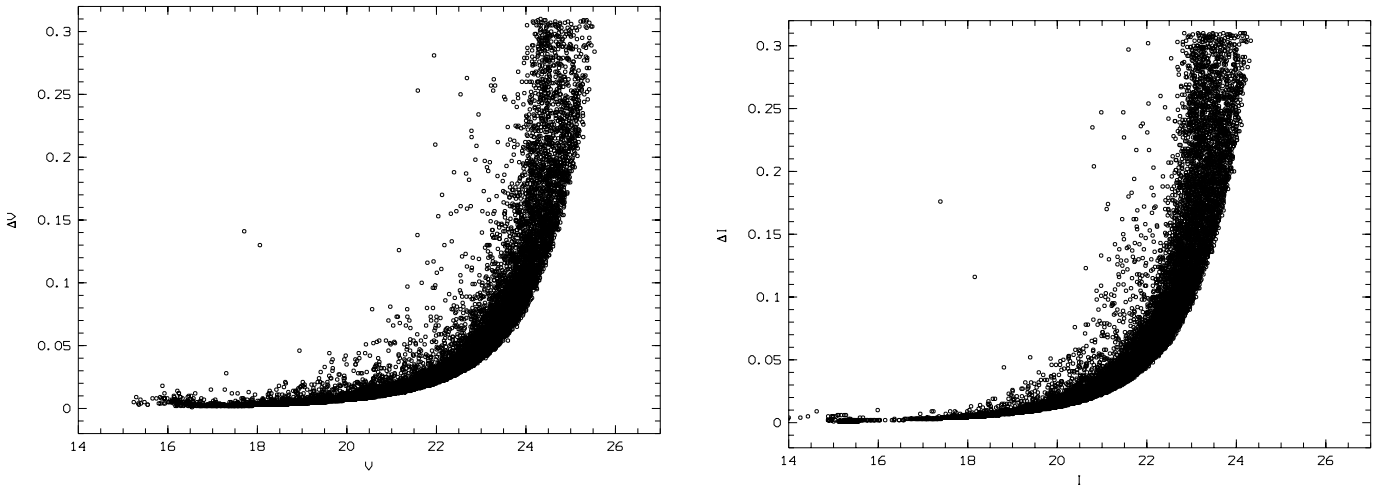

FIG. 4.—Uncertainties of PC-centered photometry as derived by HSTphot for the (*a*) F555W and the (*b*) F814W bands

The LMC field contamination has been evaluated following Stappers et al. (1997). They observed the region around NGC 1866 in an area of 668 arcmin^2 and derived the star counts of field stars in the proximity of NGC 1866. We normalized the field stars numbers to the area covered by the three WF chips plus the PC chip for a total of 5 arcmin^2, after the rejection of the pixels from 0 to 51.5 for each camera on average, as suggested by the WFPC2 handbook manual. We note that for $V < 17$ mag the field contamination is very small, thus supporting the fact that the He-burning giants (N_{RG}) quoted above refers to cluster members (within 1 σ).

The contamination of the cluster MS by the MS stars in the LMC field has been evaluated by following the same procedure. Again, we find that less than 1–2 field stars may contaminate the turnoff region. This ensures us that the conclusions about the age and evolution of the stars, obtained on the basis of the CMDs presented in this work, are not affected by LMC field stars. Since the number of field stars significantly increases toward fainter magnitudes, this contamination directly affects the luminosity function of the lower part of the MS. For this reason, we used the rescaled data by Stappers et al. (1997) to evaluate the number of LMC field stars that have to be subtracted in each bin of the luminosity functions derived from the original CMDs.

To evaluate the number of background faint galaxies that may affect our luminosity function, we adopt the data provided by Metcalfe et al. (2001). According to their work on

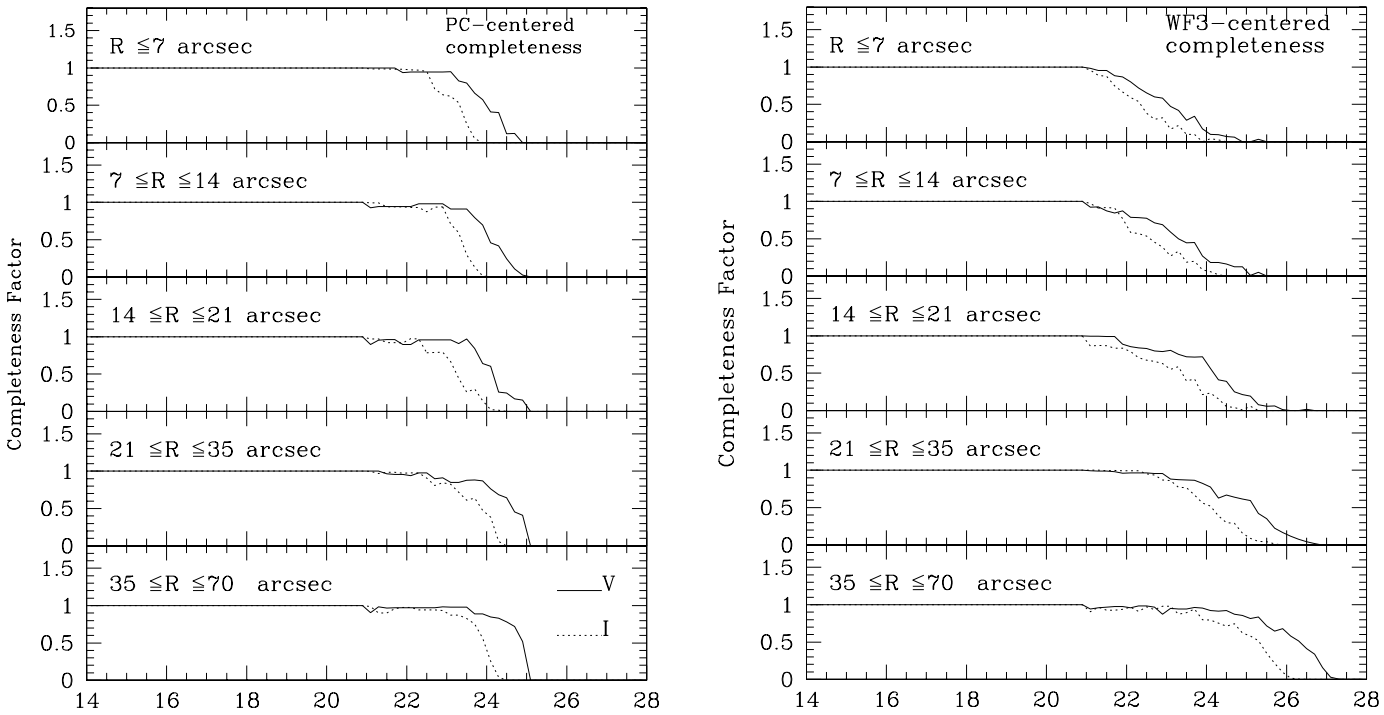

FIG. 5.—Completeness factor as obtained with the PC-centered (*left*) and WF3-centered (*right*) data sets for the labeled annuli. The curves obtained for the two photometric bands are shown.

the Hubble Deep Field, we expect a number of faint galaxies smaller than the reported uncertainties (1 σ) in each bin of the luminosity function of NGC 1866 brighter than $V \simeq 24.5$. In particular, for $V \simeq 24.5$ (bin of 0.2 mag), the number of expected galaxies in our field is of the order of $\sim$15, while the measured stars total 450 ($\pm$20). For this reason, in the following calculations we will disregard this galaxy contamination.

In summary, all the luminosity functions used in the following sections have been corrected for spurious objects, completeness, and LMC field star contamination. We have investigated possible contamination by galactic field stars and faint galaxies, and in both cases found their contributions to be negligible.

3. THE LUMINOSITY FUNCTION

We first discuss the luminosity function (LF) of the PC-centered data set, which provides firm information, particularly on the inner core region, unaffected by crowding, at least down to $V \sim 23$ mag. This limit is well below the magnitudes reached in the previous deepest ground-based observations (T99), thus allowing a substantial improvement in our knowledge of the cluster LF. Figure 6 shows the LF of the cluster MS as obtained in different annuli around the cluster center. It discloses that the shape of the LFs shows a strong dependence on the distance from the cluster center, with a clear deficiency of low-luminosity stars in the inner region. Moreover, since data in the quoted figure give the distribution of MS stars as normalized to the corresponding number of He-burning giants, one also finds clear evidence for an increasing abundance of giants when going toward the cluster center.

The problem of the origin of this observed mass segregation in NGC 1866 is beyond the scope of this paper. However, we note that strong evidence for mass segregation has recently been found by de Grijs et al. (2002) in six LMC clusters of different ages, possibly as a result of the clusters formation process. In the case of NGC 1866, Fischer et al. (1992) found a half-mass relaxation time larger than 3 Gyr for $M < 0.75\ M_{\odot}$. By following the same approach, one finds a half-mass relaxation time for the more massive stars ($\simeq 4\ M_{\odot}$) of the order of 700 Myr, i.e., still larger than the estimated cluster age (i.e., $\sim$140 Myr; see § 4) and with a core relaxation time of about 30 Myr. Thus, the observed segregation should be largely the result of an original segregation because not enough time has elapsed for relevant dynamical mass segregation outside the core, i.e., $r_c \gtrsim 14''$. It is worth mentioning that evidence of (dynamical) mass segregation has been found in the old Galactic globular clusters (e.g., Albrow, De Marchi, & Sahu 2002).

Given such an inhomogeneous spatial distribution, the problem arises of how to define a LF for the whole cluster. In the remainder of this paper, we assume that the mass segregation observed has only the effect of redistributing masses locally in the cluster without affecting the overall cluster LF (see also, de Grijs et al. 2002). Figure 2 shows that the PC-centered frames integrated with the region sampled by the WF3-centered frames cover quite a large region of the cluster, extending well beyond the half-mass radius ($\sim 50''$; Fischer et al. 1992). Thus, in the following, we will take the LF of such a sample as reasonably representative of the whole cluster. This LF (labeled as *global*) is shown in Figure 7 in comparison with the LF of the PC-centered and

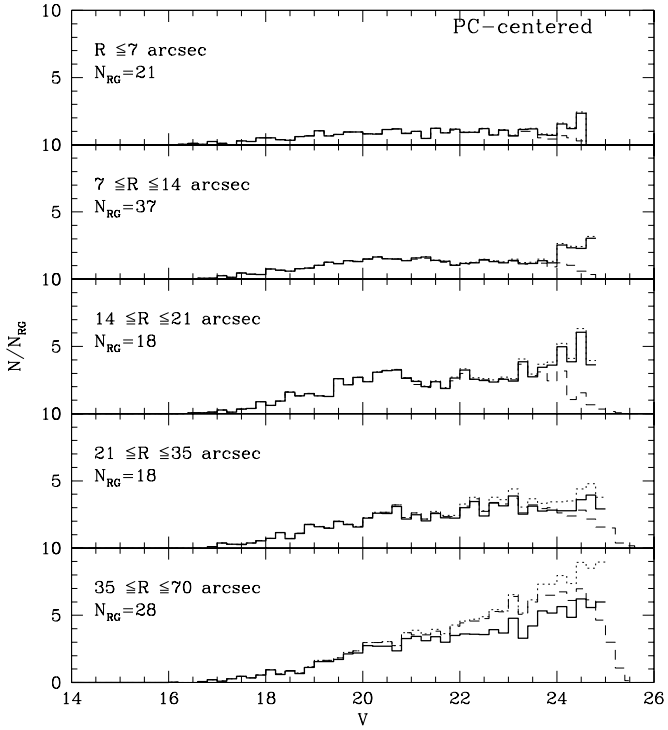

FIG. 6.—DLF normalized to the proper number of He-burning giants (RG) shown at different distances from the cluster center. The dashed lines represent the raw data after all the photometric corrections (see text), the dotted lines show the LFs after the completeness corrections, and the solid lines are the final LFs as obtained by subtracting the expected contamination of field stars.

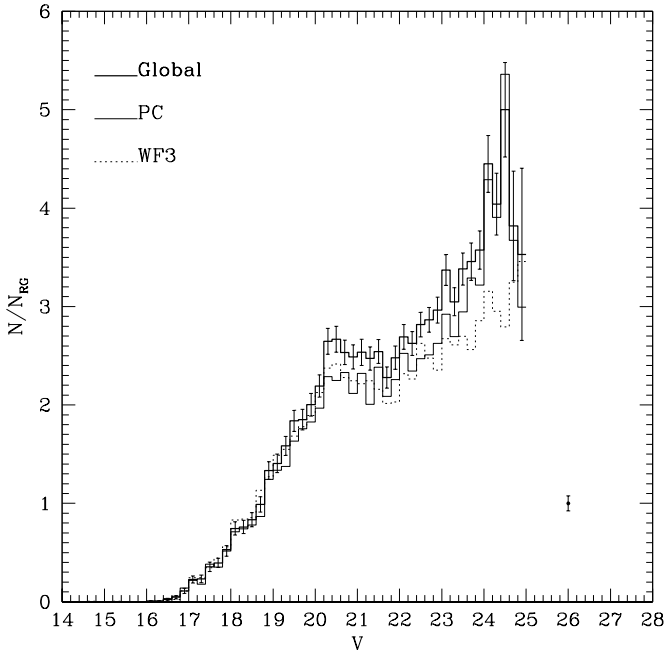

FIG. 7.—DLF of the PC (*thin solid line*) and WF3 (*dotted line*) data sets are compared after corrections due to completeness and field contaminations. Global LF (*bold solid line*) as derived by combining the observed regions of the two data sets is also shown. All the LFs are normalized to the proper number of RG stars (i.e., 128, 153, and 170, respectively). The uncertainty of the global LF due to the number of RG stars is plotted in the right bottom.

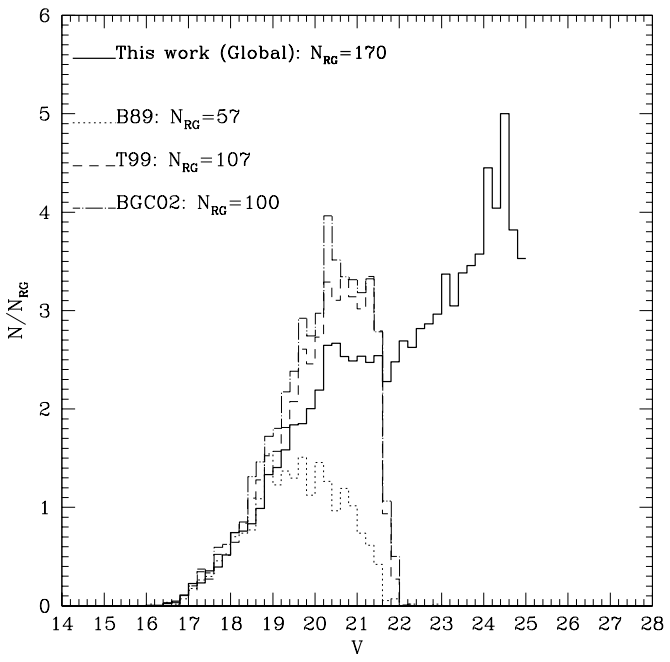

FIG. 8.—Global LF compared with the LFs derived in previous papers. The number of RG stars is also reported.

the WF3-centered data sets alone. The total number of RG stars is then $N_{\rm RG} = 170$.

Errors in the counts of stars in each bin of magnitude have been computed according to the following relation by Bolte (1989):

$$\sigma_n^2 = \left[\frac{N_{\rm obs}}{\lambda_i^2} + \frac{\sigma_{\lambda_i}^2 N_{\rm obs}^2}{\lambda_i^4} \right], \quad (1)$$

where λ_i is the completeness factor, and $N_{\rm obs}$ is the star count in the ith V bin. This formula properly considers the uncertainty due to the completeness as shown in Figure 7 for each bin value. The error due to the statistical fluctuation of the RG stars number ($\sqrt{N_{\rm RG}}$) also has to be taken into account when dealing with differential LF normalized to the RG stars. This latter error is that reported at the right bottom of the Figure 7.

Comparison with previous work in the literature, as given in Figure 8, discloses that the present LF, when normalized to the observed number of RG stars, tends to be less populated, with a difference that increases, going toward less luminous stars. This appears to be directly related to the fact that the present photometry, for the first time, measures stars to the core of the cluster, allowing investigation of the LF in this internal region.

4. THEORETICAL CONSTRAINS ON THE IMF

In order to obtain a preliminary indication on the cluster age, the left panel in Figure 9 compares the cluster CMD with the predicted distribution of star for selected assumption about the age, as evaluated assuming classical stellar models with inefficient overshooting. As in Paper I, stellar models were computed adopting the evolutionary code developed for the stellar library under construction at the University of Pisa (Castellani et al. 2003). The adopted physics input has been exhaustively described in Cassisi et al. (1998). From the results of Paper I, we assume for cluster stars $Z = 0.007$, $Y = 0.25$, and $(M - m)_V = 18.55$.

From data in Figure 9, one finds that a reasonable fit of the He-burning giants requires an age of about 140 Myr. To be conservative, in the following we will adopt as a safe estimate of the cluster age the interval $t = 100$–180 Myr. The same comparison is given in right panel of the same figure, but for models allowing a moderate overshooting (by $0.25H_P$). As is well known, one finds that increasing the amount of overshooting increases the estimated cluster age, and a reasonable fit now requires an age of the order of 200 Myr. We will assume the interval $t = 160$–250 Myr as a safe estimate of the actual cluster age if overshooting is at work. It is important to note, as found from previous similar investigations (T99; BGC02), that the age from the MS termination appears in all cases (i.e., with or without overshooting) lower than the age derived from the fitting of the luminosity of the RG stars. This is generally taken as evidence for the occurrence of a substantial number of binary stars that apparently increase the limiting luminosity of the observed MS. Table 2 gives the predicted mass of He-burning giants for the various cases, together with the mass of MS stars at two selected luminosities (see later).

In order to discuss the predicted LFs, we will adopt everywhere a logarithmic representation, which allows removal of the effect of the sample abundance, which only produces a shift along the Y-axis, keeping untouched the overall shape and slope of the distribution (Castellani, Chieffi, & Norci 1989). Figure 10 shows the predicted luminosity distribution of a suitable sample of MS stars, as evaluated with or without overshooting, a Salpeter IMF and for cluster ages covering the quoted safe intervals derived from the luminosity of He-burning giants. One finds that—in both cases (with or without overshooting) and within the safe range of ages—age can affect the distribution only above $M_V \sim 0$, whereas for fainter luminosities the distribution is determined only by the IMF. Note that, in this respect, the differential LF (DLF) we are dealing with is superior to the often adopted "cumulative" LF, where the (age-dependent) upper portion of the DLF affects the cumulative distribution even at the lower luminosities.

TABLE 2

MEAN MASSES OF HE-BURNING GIANTS AND MASSES OF MS STARS AT $M_V = 0$ AND 4.5

Age (Myr)	M(He) ($M_\odot$)	$M(M_V = 0)$ ($M_\odot$)	$M(M_V = 4.5)$ ($M_\odot$)
Classical Models			
100	4.75	3.45	1.05
140	4.15	3.30	1.05
180	3.70	3.10	1.05
Overshooting Models			
160	4.20	3.30	1.10
200	3.80	3.15	1.10
250	3.50	3.00	1.10

NOTES.—Mean masses of He-burning giants and masses of MS stars at $M_V = 0$ and 4.5 for the labeled assumptions on the cluster age and for the two different assumptions about the efficiency of overshooting. Masses are in solar masses, ages in Myr, $Z = 0.007$, and $Y = 0.25$.

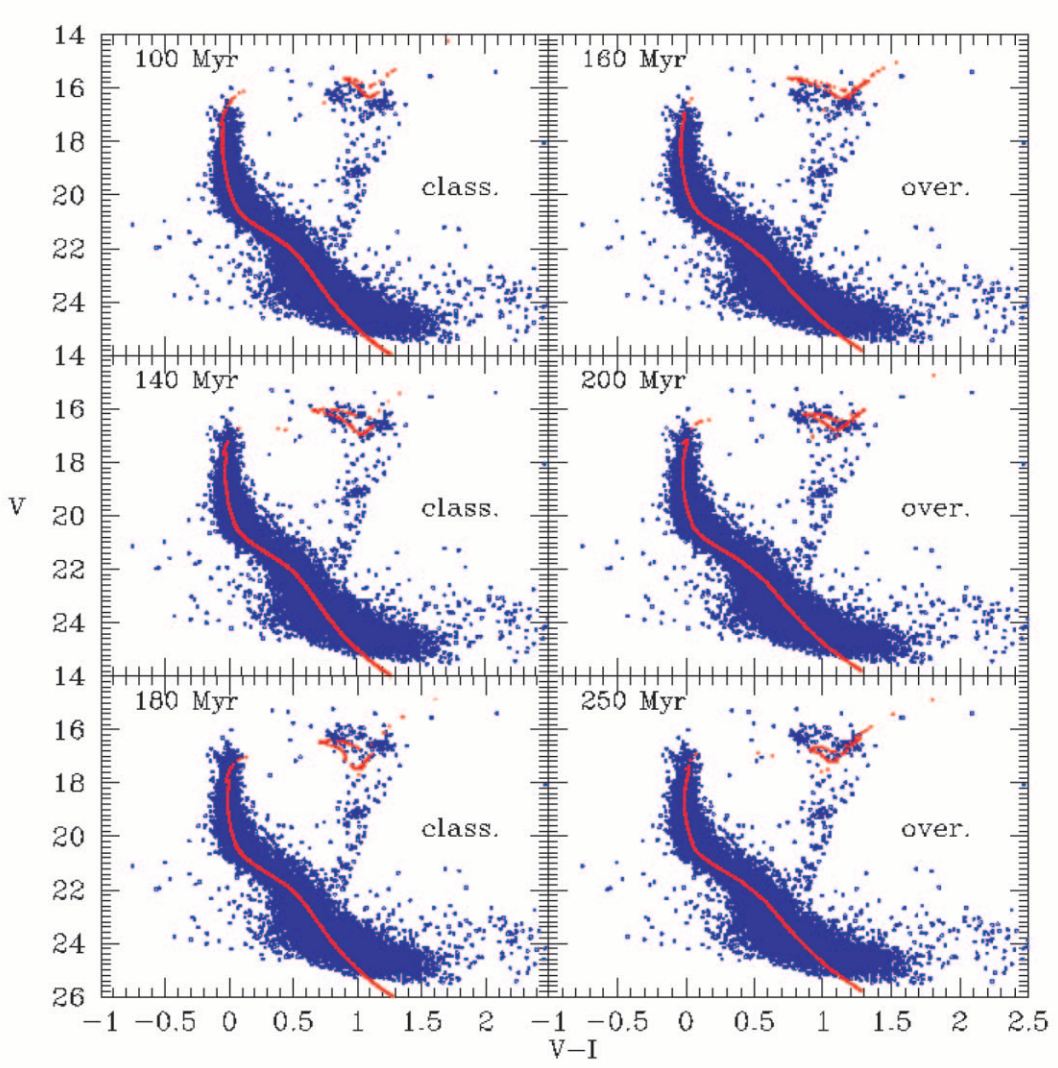

FIG. 9.—CMD of the PC-centered data set is reported (*blue dots*) and compared with the synthetic CMDs (*red dots*) computed by adopting classical (*left*) and mild-overshooting (*right*) stellar models for the labeled ages.

The predicted sensitivity to the IMF is shown in Figure 11, where we show the behavior of the DLF for a given age but for selected assumptions about the IMF exponent for classical models. As expected, one finds that assumptions about the IMF clearly modulate the behavior of the LF fainter than $M_V \sim 0$. For the given distance modulus, this means that in the magnitude interval 18.55–23 mag we directly explore the cluster IMF over an interval of more than 4 mag without the need of corrections for the completeness of the sample. In such a way, we derive information on the IMF between $M_V = 0$ and 4.5, approximately corresponding to the mass range $M = 1$–$3.5\ M_\odot$, reaching a mass of about $0.7\ M_\odot$ at the limiting magnitude $V \sim 25$.

The best fit to theoretical predictions, as given in the same figure, gives the clear evidence that in the explored range of luminosities the cluster IMF closely follows a Salpeter law. It follows that the suggestion for a larger slope, as proposed by van den Bergh (1999), is not supported by observational data, at least in the explored range of stellar masses. As quoted before, the present results rely on the hypothesis that the mass segregation present in this cluster affects the local mass distribution but not the whole cluster mass function.

Let us note that a similar result for the behavior of the IMF is also found by de Grijs et al. (2002) for a sample of six LMC clusters. As in our case, they found a radial dependence of the LF slope (then mass function) as the direct consequence of the mass segregation; the overall cluster IMF slope was found to be close to a Salpeter slope.

The fact that the LF of NGC 1866 agrees with a Salpeter mass distribution clearly affects the evaluation of the mass-to-light ratio (M/L_V). As a first point, one may recall that previous computations of the dynamical mass-to-light ratio were forced to adopt the mass function distribution as a nearly free parameter due to the lack of observations able to constraint this quantity (see, e.g., Fischer et al. 1992; van den Bergh 1999). The present results fix this question at least down to $\sim 0.7\ M_\odot$.

Although the determination of the M/L_V is not one of the scientific goals of this paper, we performed a set of simple calculations to derive the expected value by using our theoretical framework. For canonical models, adopting the age

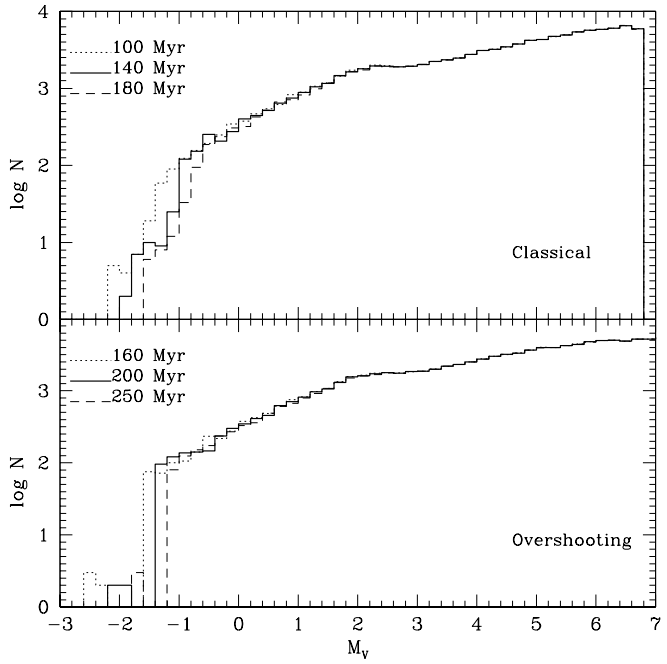

FIG. 10.—Log of the theoretical LFs derived for the labeled ages is reported. (*Top*) Classical stellar models; (*bottom*) mild-overshooting stellar models.

of 140 Myr and a Salpeter mass function in the observed range of magnitudes, we predict M/L_V values ranging from 0.17 to 0.26 (in solar units) depending on the assumption on the mass distribution function in the interval $0.1 < M/M_{\odot} < 0.5$. The higher M/L_V value corresponds to use the Salpeter mass function down to 0.1 $M_{\odot}$, while the lower value corresponds to a flatter Scalo function (Scalo 1986). In the case of overshooting, the 200 Myr best fit leads to larger values (0.20 and 0.30, respectively). As a conclusion, one finds that cluster stars experiencing nuclear burning evolutionary phases can hardly account for a M/L_V as large as 0.42. If this value will be confirmed, one cannot escape the evidence for an additional contribution to the total mass, as given by brown dwarfs or neutron stars (van den Bergh 1999).

5. OVERSHOOTING OR CLASSICAL MODELS?

For the last two decades, NGC 1866 has been often used to discuss possible evidence for the occurrence of core overshooting in the evolution of intermediate-mass stars. Owing to the controversial results appearing in the literature, we will first briefly summarize the interpretation of previous observations.

BM83 found a scarcity of He-burning giants in NGC 1866 with respect to their standard model predictions. However, Brocato & Castellani (1988) warned against making premature conclusions: the observational sample used by BM83 was severely incomplete, reaching only to $V = 18$, thus revealing only the top 1 mag of the MS, and was possibly contaminated by binaries. In addition, the BM83 stellar models did not account for either canonical semiconvection or overshooting. New V, $B-V$ photometry down to $V = 21$, including 53 He-burning giants, was presented by B89, who used improved stellar models to show that adopting the same distance modulus and the same metallicity as in BM83, i.e., $(m - M)_0 = 18.6$ and $Z = Z_{\odot}$, respectively, classical models can indeed account for the observations. However, the same year C89 presented independent observations of the cluster, producing a different LF, with a significantly larger ratio between MS and He-burning giants stars, which was taken as an evidence against standard model and in favor of overshooting.

Both samples were limited in numbers of stars, so to solve this problem Brocato, Castellani, & Piersimoni (1994, hereafter B94) took advantage of new ESO-NTT data to explore a much larger cluster region, which contained a total of 153 He-burning giants. The regions covered by the previous investigations were reanalyzed, confirming the different results, whereas the whole sample gave a LF in good agreement with B89. B94 concluded that the C89 LF was an artifact of statistical fluctuations, connected to the small number of RG stars (39) in the sample. This conclusion was further supported by the T99 reinvestigation, which with an even larger number of He-burning giants found again a LF in very good agreement with B89, concluding that classical models plus 30% of binaries nicely accounted for the observations. However, by adopting $Z = 0.008$ for the cluster metallicity, BGC02 reanalyzed the T99 data set and interpreted their results as evidence supporting core overshooting, and again invoking the occurrence of a large fraction of binary stars.

To investigate this problem, Figure 12 (*left*) compares the present LF with theoretical expectations as given for the observed 170 RG stars by models with or without overshooting. One finds that both models appear at about 4 σ from experimental data. Numerical experiments disclose that canonical model now misses the fitting just as a consequence of the new "metal-poor" composition, whereas the assumptions on the cluster distance modulus only affects the predicted cluster ages. However, the same figure shows that the presence of 40% of binaries, distributed as BGC02, moves theoretical expectations in such a way as to improve the fit, with canonical models with overshooting predictions becoming worse. As a result, the right panel in the same figure shows that, with the quoted amount of binaries and allowing for a 2 σ fluctuations on the number of RG stars, canonical models do produce a reasonable fitting. Thus, we conclude that no clear evidence against the canonical model can be found in NGC 1866.

6. FINAL REMARKS

The occurrence of uncertainties and differences in the evolutionary predictions has been often discussed in the literature and, in particular, not negligible differences in the He-burning models as computed with our or with the Padua code have been already presented and exhaustively discussed in Castellani et al. (2000). For the case of NGC 1866, we compare in Table 3 the evolutionary times during H- and He-burning phases for classical models with selected stellar masses covering the range of cluster off-MS stars.

It appears that both computations give quite similar H-burning lifetimes but differ in the He-burning phase, with Padua He-burning lifetimes being larger than in our

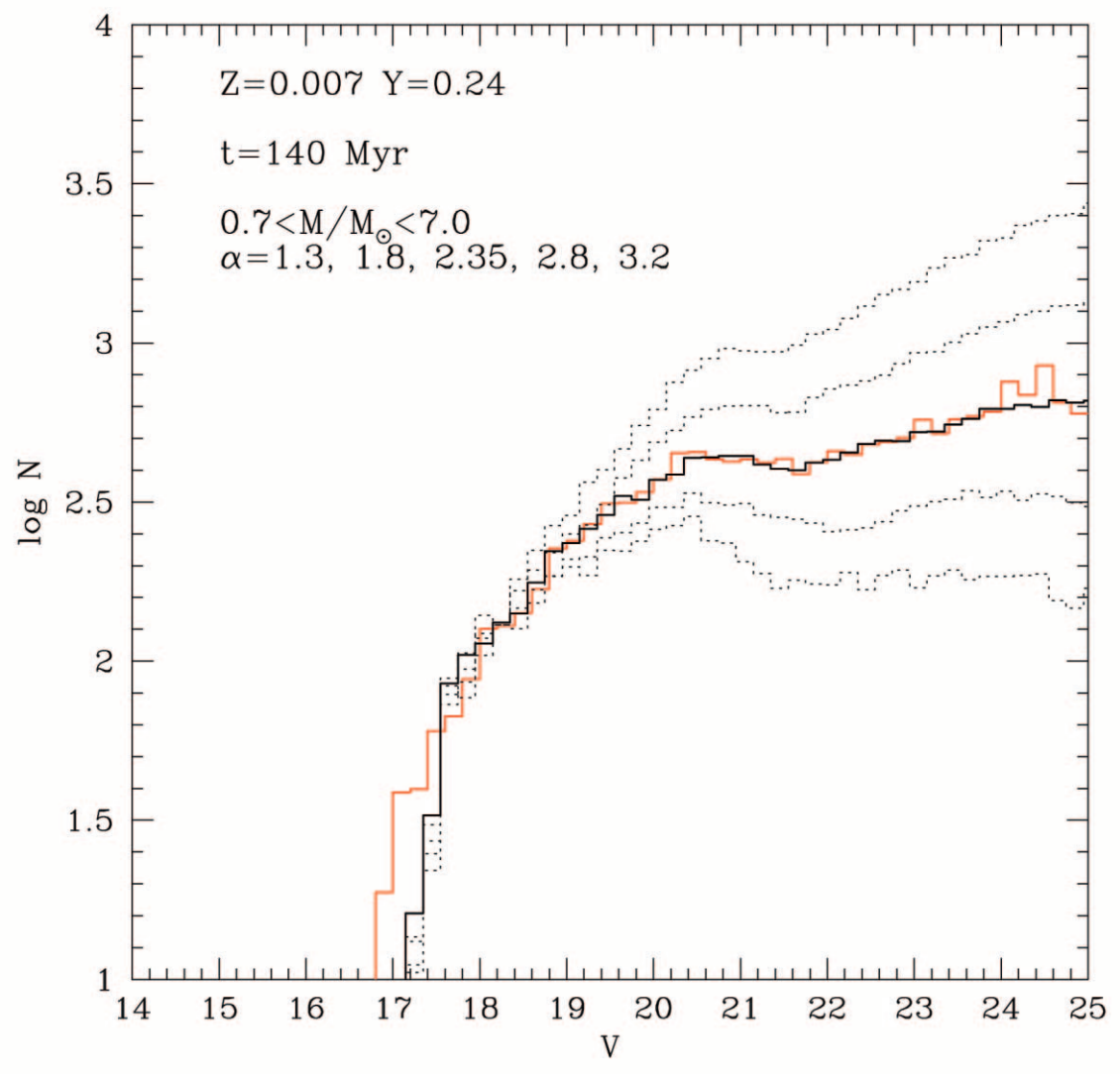

FIG. 11.—Global LF (*red line*) compared with theoretical LFs as derived by assuming the labeled values of the Salpeter exponent ($\alpha = 1 + x$) in the quoted range of masses. The solid black line refers to the value $\alpha = 2.35$.

predictions. The straightforward conclusion is that Padua computations for classical models will predict a larger number of He-burning giants and that—in that case—the introduction of overshooting as a free parameter can help in reducing the number ratio of He-burning to MS stars.

TABLE 3
SELECTED EVOLUTIONARY TIMESCALES FOR STARS WITH DIFFERENT MASS

M ($M_\odot$)	t_H (Myr)	t_{He} (Myr)	Models
3.5.....	176.9	68.0	Padua
	175.5	54.6	Pisa
4.0.....	127.1	43.2	Padua
	127.7	35.1	Pisa
5.0.....	77.5	21.9	Padua
	77.2	18.8	Pisa

NOTES.—Selected evolutionary timescales for stars with different mass as provided by the Padua group (BGC02) and the present stellar models (labeled as Pisa).

As repeatedly discussed (see, e.g., Castellani 1999), these differences originate in the use of different input physics; we cannot claim that our physics is "better," but only that our physics is fully documented in the recent literature. Thus, the most reasonable conclusion of this paper is that the new global LF can be put in agreement with our canonical model, but unfortunately NGC 1866 is in itself not sufficient to solve the controversy of whether or not overshooting is significant for these stars.

This paper is based on observations made with the NASA/ESA *Hubble Space Telescope*, obtained at the Space Telescope Science Institute, which is operated by the Association of Universities for Research in Astronomy, Inc., under NASA contract NAS 5-26555. This work is partially supported by INAF-P.R.I.N. 2002 under the scientific project Stars and Clusters as Tracers of the LMC Structure and Evolution, and by MIUR-Cofin 2002 Stellar Populations in the Local Group as a Tool to Understand Galaxy Formation and Evolution. This project made use of computational resources granted by the Consorzio di Ricerca del Gran Sasso according to the Progetto 6 Calcolo Evoluto e sue Applicazioni (RSV6)—Cluster C11/B.

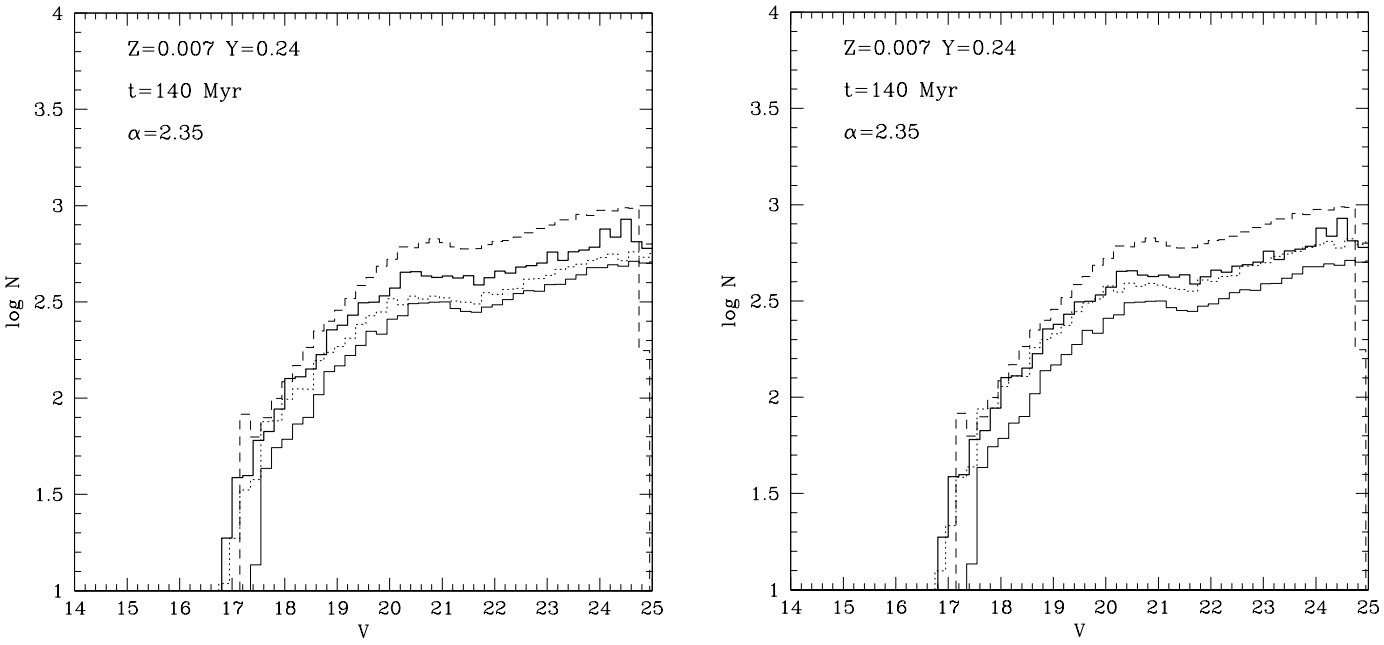

FIG. 12.—*Left*: Global LF (*bold solid line*) compared with theoretical LFs. The dashed line refers to the LF derived by mild-overshooting models. The thin solid line is the LF predicted by classical models, and the dotted line is the LF expected by classical models with the contribution of 40% of binaries (see text). *Right*: As in the left panel, but the dotted line is obtained allowing a 2 σ fluctuations of the He-burning giant stars from the LF expected by classical models with the contribution of 40% of binaries (see text).

REFERENCES

Albrow, M. D., De Marchi, G., & Sahu, K. C. 2002, ApJ, 579, 660
Arp, H., & Thackeray, A. D. 1967, ApJ, 149, 73
Barmina, R., Girardi, L., & Chiosi, C. 2002, A&A, 385, 847 (BGC02)
Becker, S., & Mathews, J. 1983, ApJ, 270, 155 (BM83)
Bolte, M. 1989, ApJ, 341, 168
Brocato, E., Buonanno, R., Castellani, V., & Walker, A. R. 1989, ApJS, 71, 25 (B89)
Brocato, E., & Castellani, V. 1988, A&A, 203, 293
Brocato, E., Castellani, V., & Piersimoni, A. 1994, A&A, 290, 59 (B94)
Cassisi, S., Castellani, V., Degl'Innocenti, S., & Weiss, A. 1998, A&AS, 129, 267
Castellani, V. 1999, in Post-*Hipparcos* Cosmic Candles, ed. A. Heck & F. Caputo (Dordrecht: Kluwer), 269
Castellani, V., Chieffi, A., & Norci, L. 1989, A&A, 216, 62
Castellani, V., Degl'Innocenti, S., Girardi, L., Marconi, M., Prada Moroni, P. G., & Weiss, A. 2000, A&A, 354, 150
Castellani, V., Degl'Innocenti, S., Marconi, M., Prada Moroni, P. G., & Sestito, P. 2003, A&A, submitted
Chiosi, C., Bertelli, G., Meylan, G., & Ortolani, S. 1989, A&A, 219, 167 (C89)
de Grijs, R., Gilmore, G. F., Mackey, A. D., Wilkinson, M. I., Beaulieu, S. F., Johnson, R. A., & Santiago, B. X. 2002, MNRAS, 337, 597
Dolphin, A. E. 2000a, PASP, 112, 1383
———. 2000b, PASP, 112, 1397
Fischer, P., Welch, D. L., Côté, P., Mateo, M., & Madore, B. F. 1992, AJ, 103, 857
Metcalfe, N., Shanks, T., Campos, A., McCracken, H. J., & Fong, R. 2001, MNRAS, 323, 795
Ratnatunga, K. U., & Bahcall, J. N. 1985, ApJS, 59, 63
Salpeter, E. E. 1955, ApJ, 121, 161
Scalo, J. N. 1986, Fundam. Cosmic Phys., 11, 1
Stappers, B. W., et al. 1997, PASP, 109, 292
Testa, V., Ferraro, F., Chieffi, A., Straniero, O., Limongi, M., & Fusi Pecci, F. 1999, AJ, 118, 2839 (T99)
van den Bergh, S. 1999, PASP, 111, 1248
Walker, A. R., Raimondo, G., Di Carlo, E., Brocato, E., Castellani, V., & Hill, V. 2001, ApJ, 560, L139 (Paper I)